

MECHANISM OF KDP GROWTH FROM SOLUTION

H. V. Alexandru^{*}, C. Berbecaru, R. C. Radulescu^a

Faculty of Physics, University of Bucharest, Romania

^aGalway-Mayo Institute of Technology, Dublin Road, Galway, Ireland

Three crystals were simultaneously grown in the same conditions, 9 liters solution volume of the crystallisation chamber, by temperature lowering method. The growth kinetic of prismatic faces was measured for a period of ~30 days. Arrhenius corrections of the growth rates were made to 55 °C growth temperature. Prismatic faces are very sensitive to Me^{3+} impurities and have typical "dead" growth zone at small supersaturations. At higher supersaturations $\sigma \geq 0.08$, 2D-nucleation mechanism becomes dominant. Using 2D-nucleation formalism introduced by Chernov [14,21] we have found the edge free energy per growth unit $\gamma = 0.39_4 kT$, in good agreement with the literature data. The coverage $\theta = 3.3 \times 10^{-6}$ of ad-molecules in the surface layer, susceptible to trigger 2D nucleation is of the same order of magnitude as Fe^{3+} impurities in solution and suggests a heterogeneous 2D-nucleation mechanism to be dominant. The lower limit of the adsorption energy ~18 kcal/mol of this impurity was estimated on the prismatic faces of KDP, much lower than ~9.5 kcal/mol the activation energy for growth. The critical coverage $\theta^* \approx 3.6 \times 10^{-4}$ at the limit of the "dead" growth zone, much higher than previous figure, suggest the segregation coefficient of this impurity increases dramatically towards low supersaturation.

(Received August 12, 2003; accepted August 21, 2003)

Keywords: Potassium dihydrogen phosphate, Solution growth, Kinetics, Mechanism of growth

1. Introduction

KDP single crystals of high quality are needed for laser fusion experiments. The laser damage threshold of the crystals depends on impurity concentration and crystal perfection, i.e. essentially on the mechanism of growth. Laser interferometry [1], and AFM [2,3] studies have shown layer growth due to dislocation and nucleation mechanisms of growth compete at $\sigma \approx 5\text{-}10\%$ supersaturation. Macroscopic growth kinetic measurements take advantage of simultaneous measurements of a number of crystals growing in the same conditions and gives statistical information about the process and the crystal quality [4-6]. The influence and the dual action of impurities on the growth kinetic of prismatic and pyramidal faces of KDP were previously presented [4,7]. New kinetic data, peculiar observations and interpretation shall be jointly presented.

2. Experimental

2.1. Growing assembly and kinetic measurements

The crystal growth equipment is presented in Fig. 1. The double walled thermostating system, fully transparent, allowed to grow and to measure simultaneously, in situ, the growth kinetics of three crystals. Crystallisation chamber of ~9 liters solution volume is placed in an outer aquarium type bath of ~30 liters distilled water, continuously stirred and thermostated ± 0.01 °C. Vertical external flat

^{*} Corresponding author: horia@alpha1.infim.ro

glasses insure a shirt of air 5 cm thick, which prevent heat losses and provide better temperature stability. A cooling water coil ("wt" in Fig. 1) can be temporarily used for temperature drop in the outer bath. Higher power heating rate can be occasionally delivered both in external bath and in the crystallisation chamber, versus the normal thermostating regime. This way a rapid stabilization of supersaturation can be normally insured. Special glass encapsulated heaters are used, which do not make solution impurification.

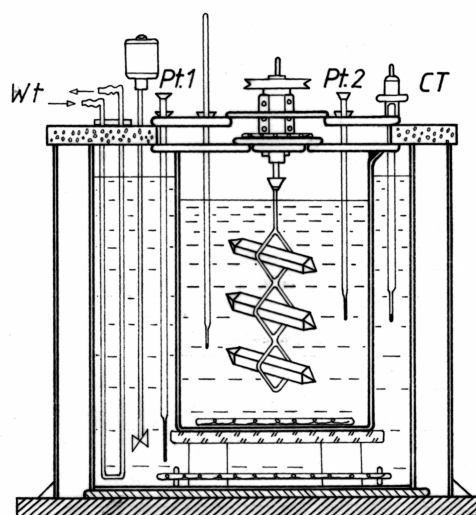


Fig. 1. The assembly for crystal growth and kinetic measurements. The double glass discs fit tightly the crystallisation chamber. In between small power heating elements compensate losses particularly at higher temperatures. Pt 1 and Pt 2 are platin 100 elements in external bath and in the crystallisation chamber.

The cover of the crystallisation chamber is double walled with glass disks and provided with special small power heaters. The cover temperature is adjusted at the limit of water condensation on the lower glass cover of the chamber. This arrangement ensures good temperature stabilization with only solution stirring produced by the "tree" with crystals.

The crystal "tree" support ensures the reversible rotation of the crystals having Z-axis in horizontal position and $\langle 110 \rangle$ crystallographic direction along the vertical rotation axis [4,7]. Reversible rotation 50÷70 rpm of the crystal "tree" (10÷30 sec every side rotation and 2÷5 sec break), electronically controlled [8], ensures the kinetic regime of growth.

Vertical dimensions R_H along $\langle 110 \rangle$ crystallographic direction and horizontal dimensions R^Z along (001) direction of the crystals could be measured with a cathetometer (± 0.01 mm). The mean growth rate values of the prismatic faces were estimated as $R^{(100)} = R_H / 2\sqrt{2}$ for every crystal. The supersaturation was adjusted with the aid of the temperature program.

2.2. Electronic equipment for temperature program

The electronic equipment for temperature control includes a micro-computer and a parallel interface, a phase control power regulator and a time-temperature recorder, see Fig. 2. The digital (Platin 100) thermometer performs two readings per second and the temperature accuracy control is ± 0.01 °C, on the temperature range 10÷100 °C. All electronic components were connected via the 8 bit parallel interface. The feeding of the microcomputer and the digital thermometer was made in line with a DC -12 volts storage battery, to prevent disturbances due to accidental break of electric power. Two platin 100 Ω sensors, specially calibrated, were used. One sensor ensure the thermostatisation in the outer bath, the other one can read the actual temperature in the crystallisation chamber, when it is inquired on purpose.

The computer temperature program, with 32 steps ensures a flexible monitoring of the growth parameters, according to the growth regime or kinetic measurements. A large graphic of the leading

parameters (growing temperature, saturation point evolution, crystals dimension, estimated supersaturation, growth rates, etc) is completed every day. Kinetic data, growth rates versus supersaturation finally emerge. Some other specific observations are also important: stirring rates, period of the rotation reversal and the break, in relation with crystals dimension and hydrodynamic of the system. Arrhenius correction to 55 °C were made for all growth rates measured at lower temperatures, using the activation energy of $\Delta G = 9.5$ kcal/mol. We have previously used this figure for KDP growth [4], in good agreement with Chernov and Rashkovich [9].

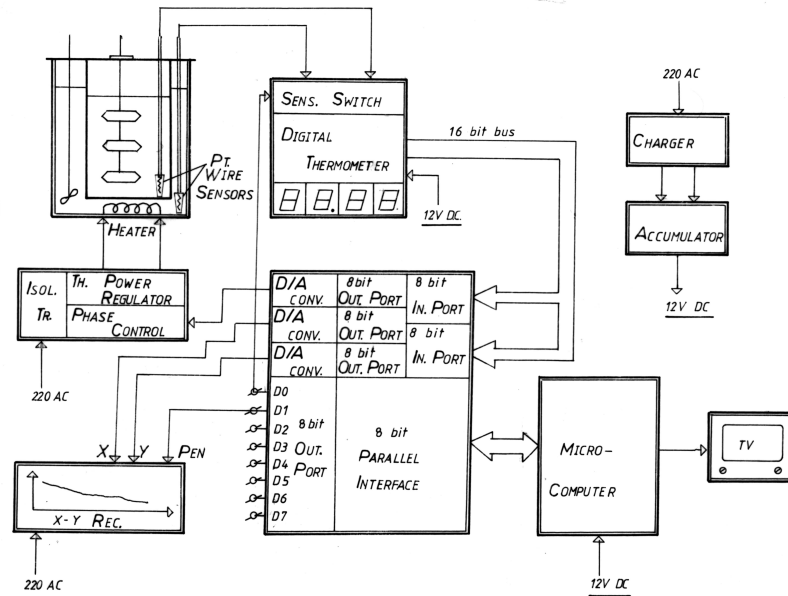


Fig. 2. The design of the crystal growth equipment and the electronic temperature control system. The digital thermometer and microcomputer are 12 V - DC fed in line with an accumulator, to prevent large voltage variation or small electrical power break.

2.3. Solution, seeds and supersaturation

Z-cut seeds, closely shaped to the natural habit of the crystal, were firmly attached to the "tree" support with nylon wires [7]. Seed regeneration was usually completed in two hours at higher supersaturations. Kinetic measurements at several supersaturations were realized by temperature reduction during about thirty days. The supersaturation was controlled by temperature adjustment.

A double fractional recrystallisation procedure [10-12] was used to improve the quality of raw KDP material. The middle fraction of the final product was used for solution preparation. Emission and atomic absorption spectroscopy have shown $\text{Fe}^{3+} \approx 10$ ppm, the major impurity in this fraction.

The mole fraction concentration in solution was fitted by equation [4,6]:

$$C^{mf}(T) = C_{\infty}^{mf} \exp(-\Delta H_{diss} / RT) \quad (1)$$

where at normal pH ~ 4 , $C_{\infty}^{mf} = 15.17$ and the dissolution enthalpy $\Delta H_{diss} = 3.656$ kcal/mol, is constant on a large temperature interval 20÷60 °C. We have used the reference data [4,13].

The concentration X (g KDP/100g H₂O), useful in solution preparation was calculated according to the formula [6]:

$$X(T) = 755.4_1 \left[\frac{1}{C^{mf}(T)} - 1 \right]^{-1} \quad (2)$$

The supersaturation we shall use in this paper is defined [4,6]:

$$\sigma = \sigma^{\ln C} = \frac{\Delta\mu}{RT} = \ln \frac{C^{mf}}{C_E^{mf}} = \frac{\Delta H_{diss}}{RT_S} \sigma^T \tag{3}$$

where $\Delta\mu$ is the chemical potential variation of the solute and C^{mf} , C_E^{mf} are actual and equilibrium mole fraction concentrations. These concentrations correspond to T_S -the saturation temperature, T_E - the actual temperature and $\sigma^T = (T_S - T_E)/T_E = \Delta T / T_E$.

3. Results

Vertical dimensions R_H of the tree crystals were measured in situ with a cathetometer along $\langle 110 \rangle$ crystallographic direction at several supersaturations. Examples of crystal dimension variation at constant supersaturations are presented in Fig. 3.

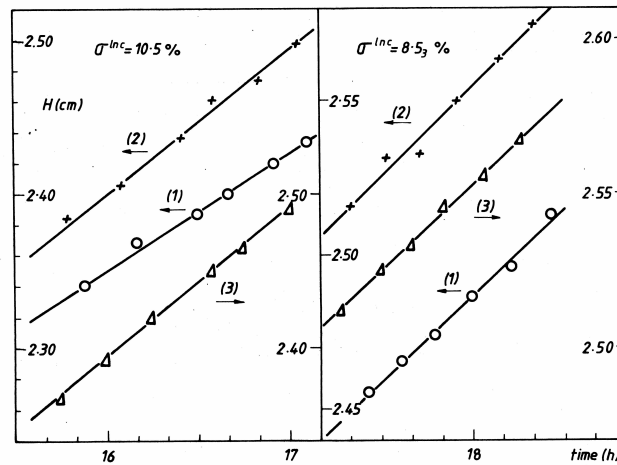


Fig. 3. The increase of KDP prismatic face dimensions, measured along the $\langle 110 \rangle$ direction, at two constant supersaturation values. The figures in parentheses shows the crystal number on the “tree” support and arrows show the left or the right hand side scales.

The measured growth rate R_H of the prismatic faces was drawn versus the supersaturation in double log scale in Fig. 4. Two distinct mechanism of growth in regions “c” and “b” are clearly seen and a transient region “a” towards the “dead” growth zone at smaller supersaturations is suggested.

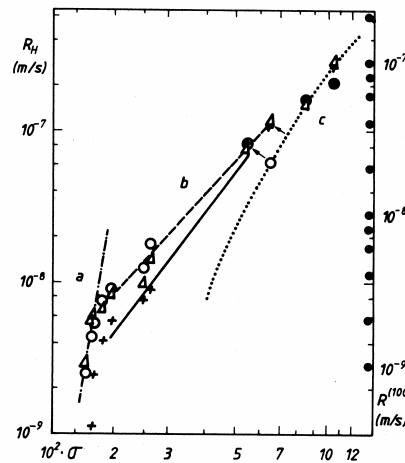


Fig. 4. Growth kinetic data $R - \sigma$ in double log scale. Three distinct regions of growth kinetic can be followed: c/ 2D nucleation mechanism, b/ dislocation mechanism, a/ transient region towards the “dead” growth zone.

3.1. Two-dimensional nucleation mechanism (region “c”)

In Fig. 5 we have represented all kinetic data in the coordinates of 2D nucleation mechanism.

At higher supersaturations, in the region “c”, the 2D-nucleation mechanism is expected to become dominant and according to Malkin et al [14], equation:

$$R_H = A_H \sigma^{5/6} \exp\left(-\frac{B}{\sigma}\right) \Rightarrow \ln \frac{R_H}{\sigma^{5/6}} = \ln A_H - \frac{B}{\sigma} \quad (4)$$

is valid, where A and B are constants, shall be further discussed (upper representation in Fig. 5).

An earlier equation for two dimensional nucleation theory of growth [15] we have also represented in Fig. 5:

$$R_H' = \frac{kT}{h} K^\ddagger d \cdot \exp\left[-\pi \left(\frac{\gamma'}{kT}\right)^2 \frac{1}{\sigma}\right] \quad (5)$$

where (kT/h) is the frequency factor, K^\ddagger activation entropy factor, d interplanar distance and γ' the edge free energy of the growth unit (GU) in the step.

Growth kinetic data for the tree crystals are presented according to eqs. (4) and (5) in Fig. 5. Both versions show the same distinct regions of growth as in Fig. 4.

From region “c” of upper representation in Fig. 5, constants $A_H = 4.84_4 \cdot 10^{-6}$ m/sec and $B = 0.16_{25}$ in eq. (4) were found. Using the formalism from refs. [1,4,14,17], from B constant in eq. (4):

$$B = \frac{\pi}{3} \left(\frac{\gamma'}{kT}\right)^2 \quad (6)$$

the edge free energy ratio per GU in the steps $\gamma'/kT = 0.39_4$ could be found. This figure is in very good agreement with the values $0.39_1 \div 0.39_4$ estimated by Söhnel et al [16] and 0.41 estimated by Alexandru et al [4]. This figure corresponds to the surface energy $\alpha \approx 12$ mJ/m².

In the region “c” the lower representation in Fig. 5 of eq. (5) is given by:

$$R_H' (m/s) = 1.94_5 \cdot 10^{-6} \exp\left(-\frac{0.24_9}{\sigma}\right) \quad (7)$$

and the edge free energy ratio of the GU found $\gamma'/kT = 0.28_2$ is smaller than previous value.

3.2. Dislocation mechanism of growth (region “b”)

Using the experimental data from Fig. 4, an empirical equation $R_H = K \cdot \sigma^n$ fit the data in the region “b”. If we consider the BCF –dislocation mechanism of growth [18], the exponent has to be $1 < n < 2$. For solid and broken lines in Fig. 4, the exponent values are 2.65 and 2.20 respectively. The dispersion of the kinetic data around $\sigma \sim 2$ % in Fig. 4 explain this dispersion of the exponent, in connection with activity of the dominating center of dislocations [19,20]. The super-parabolic dependence of the growth rates on supersaturation cannot be explained in the frame of the BCF theory. However, as previously shown [4,20], a possible explanation is the step retardation effect due to stopper impurities, whose effect increases rapidly towards smaller supersaturations (see section 4).

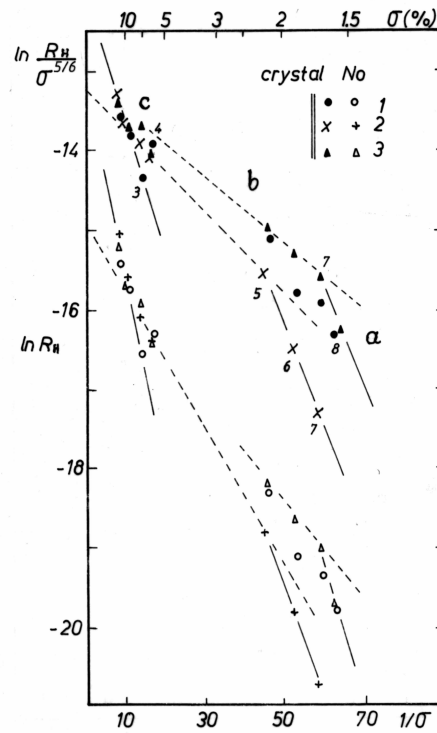


Fig. 5. Kinetic data in coordinates of the nucleation mechanism of growth. Upper and lower representation correspond to eq. (4) and to eq. (5), respectively (see text).

3.3. Retardation effect of impurities (region "a")

The region "a" is a transient one towards the "dead" growth zone at smaller supersaturations, where no measurable growth rate occurs due to impurities. The sensitivity limit of our measurements $\sim 10^{-10}$ m/sec (± 0.01 mm / 24 hours) is comparable with the sensitivity limit of laser interferometry 3×10^{-11} m/sec [14]). In this region, the edge free energy ratio $\gamma / kT = 0.44 \div 0.49$ is comparable with the value found in the region "c". However, A_H constant in eq. (4) is about four orders of magnitude higher than in the region "c". The corresponding coverage $\vartheta = n_s / n_0 \gg 1$ has no physical support and shows the 2D nucleation model do not apply in the region "a" (section 4).

4. Discussion

Following the same procedure as in refs. [4,7,14], we have used the constant value from eq.(4): $A = A^{(100)} = A_H / 2\sqrt{2} = 2.06_6 \times 10^{-6}$ m/s and we have found the surface density of adsorbed molecules on the crystal surface, susceptible to produce 2D nucleation:

$$n_s = \frac{(A / C_e \beta_\ell)^3}{\omega^2 d^4 \bar{a}} = 1.27_7 m^{-2} \quad (8)$$

We have used the following data and kinetic parameters:

- $C_e^{55^\circ C} = 1.65 \times 10^{27} m^{-3}$ - the equilibrium volume concentration of GU in solution, calculated according to the solubility curve [7].
- The kinetic coefficients of steps in the equation of step velocity $v = \beta_\ell C_e \omega \sigma$, estimated according to equation [14,21]: $\beta_\ell = \bar{a} (kT / h) \exp(-E_\beta / RT) = 1.19_6 \times 10^{-3} m / sec$, where

$E_\beta = 9.7 \text{ kcal/mol}$ [9] is the activation energy for step motion, $kT/h = 6.83 \times 10^{12} \text{ sec}^{-1}$ is the frequency factor and $\bar{a} = 5.08_6 \times 10^{-10} \text{ m}$ is the mean linear dimension of the GU on the prismatic faces.

- $\omega = 9.61_7 \times 10^{-29} \text{ m}^{-3}$ - the volume of the GU in the KDP lattice and
- $d = a_2/2 = 3.71_7 \times 10^{-10} \text{ m}$ - the elementary step high.

The coverage of these ad-molecules in the surface layer can be estimated:

$$\theta = \frac{n_s}{n_o} = 3.3 \times 10^{-6} \quad (9)$$

where $n_o = (\bar{a})^{-2} = d/\omega = 3.86_5 \times 10^{-18} \text{ m}^{-2}$ is the surface density of native molecules in KDP lattice on the prismatic faces. Because the relative concentration of adsorbed molecules on the crystal surface, susceptible to trigger the 2D nucleation mechanism $\theta \ll 1$, it may be supposed the nucleation mechanism is heterogeneous. Indeed, the main impurity in the basic substance Fe^{3+} was found by spectroscopic analysis in concentration of ~ 10 ppm. If we take into account the segregation coefficient $K_{\text{Fe}} = 0.5$ found by Belouet [22], the surface coverage eq. (9) is almost the same as the relative impurity concentration in crystal, i.e. ~ 5 ppm.

This fact suggest the life time τ of Fe^{3+} impurity in the adsorption layer is very long compared with the time interval $t_1 = d/R^{(100)}$ between two successive steps crossing a point on the crystal surface. Thus, at the limit, we have the following correlation:

$$t_1 = \frac{d}{R} \leq \tau = \left(\frac{kT}{h}\right)^{-1} \exp\left(\frac{E_{ads}}{kT}\right) \quad (10)$$

Using the extreme values of the growth rates in Fig. 4, $R^{(100)} \approx 10^{-7} \div 10^{-9} \text{ m/s}$ and the elementary step high $d = 3.71_7 \times 10^{-10} \text{ m}$, we find at the limit of eq. (10) the minimum values of the activation energy of adsorption of impurities $15.6 \div 18.6 \text{ kcal/mol}$ respectively. Thus, this values are much larger than the activation energy for growth $\sim 9.5 \text{ kcal/mol}$ [4] (the dehydration step of the GU which enter the surface layer). Adsorption energy of impurities as large as 24 kcal/mol was estimated by Chernov and Malkin [25,26] for pyramidal faces of ADP. The “life” time in the adsorbed layer for such impurity is of the order $\tau \sim 5 \times 10^4 \text{ sec}$, i.e. much larger than $t_1 \sim (10^{-3} \div 10^{-1}) \text{ s}$ in our experiments.

At lower supersaturations such impurities play the role of stopper for elementary steps produced by the dislocation mechanism on the crystal surface and finally are “engulfed” in the crystal lattice. At higher supersaturations, heterogeneous 2D-nucleation plays an important role, exceeding the homogeneous 2D-nucleation. Individual impurities having a high energy of adsorption, which did not actually initiate nucleation, still play the role of stoppers. However, increasing the supersaturation, the time between two successive steps $t_1 = d/R^{(100)}$ crossing a point on the crystal surface become shorter and impurities concentration in the adsorbed layer decreases continuously. This way, although paradoxically, the impurity concentration in the crystal have to decrease at higher growth rates. This is in strong contrast with the behavior of the segregation coefficient in melt growth of crystals [24].

There is another aspect which worth to be mentioned. At lower supersaturations, at the limit of the “dead” growth zone, the critical coverage θ^* is related to the critical supersaturation $\sigma^* \sim 1.5\%$ by the relation:

$$\theta^* = \frac{n_s^*}{n_o} = \left[\frac{\bar{a}}{2\rho^*}\right]^2 = \left[\left(\frac{\gamma}{kT}\right)\frac{2}{\sigma^*}\right]^{-2} \approx 3.6 \times 10^{-4} \quad (11)$$

Indeed, in view of Cabrera-Vermilyea concept [23], the surface layers extension on the crystal surface is completely stopped, when the mean distance between stopper impurities is smaller than the

diameter of the critical nucleus $2\rho_c^* = 2(\gamma/kT) \cdot (\bar{a}/\sigma^*)$. At this stages the elementary steps cannot squeeze any longer through the “forest” of stoppers on the crystal surface and the growth is completely stopped. The critical coverage in eq. (11) $\theta^* \approx 3.6 \times 10^{-4}$, which is in good agreement with the value found in ref [7], is two orders of magnitude higher than the ordinary coverage $\theta = 3.3 \times 10^{-6}$ estimated in eq. (9).

This fact suggests the retarding effect of impurities monotonously increases at smaller supersaturations and consequently the segregation coefficient increases very rapidly towards the smaller supersaturations. The unusual value $n = 2.20 \div 2.65$ of the exponent in equation $R_H = a \sigma^n$ corresponding to region “b” can be understood if the substantial decrease of the growth rates are taken into consideration at smaller supersaturations.

Finally, we shall consider the region “c” and the characteristics of 2D critical nucleus.

In the supersaturation region $\sigma = (7 \div 10) \%$, where $\gamma/kT = 0.39_4$ was estimated, the critical radius corresponding to 2D nucleation mechanism is:

$$\rho^* = \frac{\gamma}{kT} \frac{\bar{a}}{\sigma} \approx (4 \div 6) \bar{a} \quad (12)$$

where $\bar{a} = 5.08_6 \times 10^{-10}$ m is the mean linear dimension of the growth units on the prismatic faces of KDP. This corresponds to about 50÷100 GU in the critical 2D nucleus and appears to be in good agreement with the classical theory of nucleation.

5. Conclusions

Growth mechanism of the prismatic faces of KDP have been analysed on a large supersaturation range. Dislocation mechanism of growth is heavily affected, particularly towards the smaller supersaturations. 2D-nucleation mechanism of growth become dominant at higher 8÷10 % supersaturations.

The estimated coverage of ad-molecules in the surface layer, susceptible to trigger 2D-nucleation mechanism is $\theta = 3.3 \times 10^{-6}$. This figure is too small to be considered as a true coverage of native ad-molecules in homogeneous 2D-nucleation. The figure is close to the value of relative concentration of the major impurity Fe^{3+} (≈ 10 ppm) in the growing solution. Considering the segregation coefficient 0.5 of this impurity, as found by Belouet [22], the concentration in crystal is very close to the coverage we have estimated in the surface layer of the crystal.

The minimum value of the adsorption energy estimated for this impurity, of about 18 kcal/mol is much higher than the activation energy for growth ~ 9.5 kcal/mol. The critical coverage of impurities at the limit of the “dead” growth zone $\theta^* \approx 3.6 \times 10^{-4}$, suggests the segregation coefficient of this impurity dramatically increases towards smaller supersaturation.

References

- [1] A. A. Chernov, *Contemp. Physics* **30**, 251 (1989).
- [2] J. J. De Yoreo, T. A. Land, B. Dair, *Phys. Rev. Letters* **73** (6), 838 (1994).
- [3] J. J. De Yoreo, T. A. Land, J. D. Lee, *Phys. Rev. Letters* **78** (23), 4462 (1997).
- [4] H. V. Alexandru, C. Berbecaru, Al. Grancea, V. Iov, *J. Cryst. Growth*, **166**, 162 (1996).
- [5] H. V. Alexandru, *J. Cryst. Growth*, **169**, 347 (1996).
- [6] H. V. Alexandru, *Anal. Univ. Buc.* **46**, 9 (1997), Proceedings of the conf. ROCAM '97, Romanian Academy, Nov. 24-26, 1997.
- [7] H. V. Alexandru, *Cryst. Res. Technol.* **30**, 1071 (1995).
- [8] H. V. Alexandru, C. Berbecaru, M. Ionila, Al. Grancea, B. Logofatu, *Anal. Univ. Buc.* **44**, 11 (1995).
- [9] A. A. Chernov, L. N. Rashkovich, *J. Crystal Growth* **84** 389 (1987).
- [10] H. V. Alexandru, A. C. Otea, G. Hlevca, *Rev. Roum. Phys.* **30**, 525 (1985).

-
- [11] H. V. Alexandru, C. Berbecaru, *Cryst. Res. Technol.* **30**, 307 (1995).
- [12] H. V. Alexandru, C. Berbecaru, B. Logofatu, Anca Stanculescu, F. Stanculescu, *J. Optoelectron. Adv. Mater.* **1** (4), 57 (1999)
- [13] J. W. Mullin, A. Amatavivadhana, M. Chakraborty, *J. Appl. Chem.* **20**, 153 (1970).
- [14] A. I. Malkin, A. A. Chernov, I. V. Alexeev, *J. Cryst. Growth* **97**, 765 (1989).
- [15] P. Bennema, thesis, University of Groningen, 1965.
- [16] O. Söhnel, J. Garside, S. J. Jancic, *J. Cryst. Growth* **39**, 307 (1977).
- [17] P. Bennema, J. Boon, C. van Leeuwen C., G. H. Gilmer, *Kristall und Technik* **8**(6), 659 (1973).
- [18] W. K. Burton, N. Cabrera, F. C. Frank, *Phil. Trans. R. Soc. London A* **243**, 299 (1951).
- [19] H. V. Alexandru, C. Berbecaru, 14-th International Symposium on Industrial Crystallization, 12-16 sept.1999, Cambridge, UK, abstr. pag. 99, Proceedings 282 (3).
- [20] H. V. Alexandru, *J. Crystal Growth* **205**, 215 (1999).
- [21] A. I. Malkin, A. A. Chernov, I. V. Alexeev, *Kristallographiya* **34**(4), 968 (1989).
- [22] C. Belouet, *Acta Electron.* **16**, 345 (1973).
- [23] N. Cabrera, V. A. Vermilyea, in "Growth and Perfection of Crystals", New York 1958, pag.393.
- [24] A. A. Chernov, "Modern Crystallography III – Crystal Growth", Springer-Verlag, 1984.
- [25] A. A. Chernov, A. I. Malkin, I. L. Smol'skii, *Kristallografiya* **32**(6), 1508 (1987).
- [26] A. A. Chernov, A. I. Malkin, *Kristallografiya* **33**(6), 1487 (1988).